Intermetallics 57 (2015) 83–92

Contents lists available at ScienceDirect

Intermetallics

journal homepage: www.elsevier.com/locate/intermet

Effects of B addition on the microstructure and properties of Nb silicide based ultrahigh temperature alloys

Song Zhang, Xiping Guo*

State Key Laboratory of Solidification Processing, Northwestern Polytechnical University, Xi'an 710072, PR China

ARTICLE INFO

Article history:
Received 28 June 2014
Received in revised form
17 September 2014
Accepted 14 October 2014
Available online 5 November 2014

Keywords:
A. Silicides, various
B. Oxidation
B. Fracture toughness
D. Microstructure
F. Electron microscopy, scanning

ABSTRACT

Four Nb silicide based ultrahigh temperature alloys with compositions of Nb–22Ti–16Si–5Cr–4Hf–3Al–xB (x = 0, 2, 5 and 10, respectively) (at%) were prepared by vacuum non-consumable arc melting. The effects of B content on the phase selection, microstructure, oxidation resistance at 1250 °C, room-temperature fracture toughness and microhardness of the alloys were investigated. The results showed that the microstructures of the four alloys were all comprised of primary silicide blocks, Nbss dendrites and eutectic colonies. However, the crystal structures or types of silicides and the amounts of constituent phases obviously varied with increase in B content in the alloys. The oxidation resistance of the alloys was significantly ameliorated by B addition. The room temperature fracture toughness of the alloys was improved with 2 at% B addition but degraded with 5 or 10 at% B addition. The microhardness of Nbss rose slightly with increase in B content in the alloys, while that of silicides was dependent on their crystal structures, types and concentrations of alloying elements.

1. Introduction

Development of aero-technology promotes the requirements for turbine blade materials of aeroengine with excellent and balanced properties, such as good room-temperature fracture toughness, exceptional high temperature endurance strength, creep rupture strength and oxidation resistance [1,2]. In recent years, the temperatures experienced by high pressure turbine blade materials have approached to ~1150 °C, which is essentially close to the limit for Ni based single crystal superalloys [3]. Further increase in the temperature capability of these Ni based superalloys will be difficult to achieve due to their relatively low melting points (~1350 °C). Therefore, new high temperature structural materials that can survive between 1200 and 1400 °C for long time are desired. Nb silicide based ultrahigh temperature alloys (namely Nb silicide based *in situ* composites) that comprise of Nbss, $(Nb,X)_5Si_3$ or $(Nb,X)_3Si$ and sometimes $Cr_2(Nb,X)$ ('X' represents Ti, Hf, Cr and V etc., which generally substitute for Nb in the lattices), have been shown to possess great potential as alternative materials to Ni based superalloys due to their high melting points (above 1750 °C), low density (6.6–7.2 g/cm^3) and preferable room and high temperature mechanical properties [4,5]. However, their relatively poor oxidation resistance at high temperatures is a major barrier to applications of these alloys in the field of aerospace [1–5].

In order to improve the integrated properties of Nb silicide based ultrahigh temperature alloys, especially their oxidation resistance, multi-alloying has been employed. Alloying elements added in Nb–Si alloys are mainly Ti, Cr, Al, Sn, Mo, W, Hf, V, B, Ta, Fe, Zr and C etc. [6–20]. The additions of Ti, Cr, Al and Sn to Nb silicide based ultrahigh temperature alloys can improve their oxidation resistance [6–10]. However, the elements Cr and Al destabilizing $(Nb,X)_3Si$ will bring deleterious effect on the room-temperature fracture toughness and ductility [7,11,12]. Alloying with Mo and W can stabilize $\beta(Nb,X)_5Si_3$ (tetragonal $D8_m$, W_5Si_3-type structure) and strengthen these alloys by solid solution hardening [13–15]. The addition of Hf in Nb silicide based ultrahigh temperature alloys can improve their oxidation resistance and cause the formation of $\gamma(Nb,X)_5Si_3$ (hexagonal $D8_8$, Mn_5Si_3-type structure) [9,10,13]. Alloying with V can stabilize $\alpha(Nb,X)_5Si_3$ (tetragonal $D8_l$, Cr_5Si_3-type structure) by increasing the c/a value and make the 0.2% offset yield strength at room temperature increase [20].

In recent years, B as a modifying element in metallic materials (especially in intermetallics) has been widely concerned by researchers. The addition of B in Nb silicide based ultrahigh temperature alloys is effective in terms of refining crystal grains, stabilizing $\alpha(Nb,X)_5Si_3$ and ameliorating room-temperature fracture toughness [16–19]. Nevertheless, the effects of B on the high-temperature oxidation resistance of these alloys have been rarely

---

* Corresponding author. Tel./fax: +86 29 88494873.
E-mail address: xpguo@nwpu.edu.cn (X. Guo).

http://dx.doi.org/10.1016/j.intermet.2014.10.007
0966-9795/© 2014 Elsevier Ltd. All rights reserved.

studied. Furthermore, researches on alloying with B mainly focused on simple binary, ternary and quaternary systems (such as Nb–Si, Nb–Ti–Si and Nb–Mo–W–Si etc.). Thus, further study is required. This paper has concentrated on the effects of B content on phase selection, microstructure, oxidation resistance, room-temperature fracture toughness and microhardness of the alloys based on multicomponent Nb–Ti–Si–Cr–Hf–Al system.

2. Experimental procedures

Four ingots of Nb silicide based ultrahigh temperature alloys with compositions of Nb–22Ti–16Si–5Cr–4Hf–3Al–xB ($x = 0$, 2, 5 and 10 respectively, and the alloys are respectively referred to 0B, 2B, 5B and 10B alloys hereafter) (at%) were prepared by vacuum non-consumable arc-melting under an argon atmosphere. The ingots were remelted for six times in order to ensure compositional homogeneity. Specimens used for microstructural analysis and oxidation tests were cut into $8 \times 8 \times 8$ mm^3 cubes by electro-discharge machining (EDM). After their six surfaces being ground using SiC-grit abrasive papers up to 1200#, the specimens used for oxidation tests were cleaned in an ultrasonic acetone bath and then dried. Furthermore, the actual dimensions of each specimen were measured and their surface areas were calculated before the oxidation tests.

The alloys with different B contents were examined for their oxidation resistance by heating them in an open-ended tube electric furnace in static air. The specimen was placed in an alumina crucible, and thus the total mass change of the crucible set including possibly spalled scales could be obtained. Once the crucible was set in, the furnace was firstly heated up to 450 °C at a rate of 10 °C/min, and then the temperature was further raised at a rate of 27 °C/min to 1250 °C. After holding the specimens at 1250 °C for 1 or 50 h, the furnace was cooled down to room temperature at a rate of 5 °C/min. The mass changes of the specimens after oxidation tests were weighed in an electronic balance with an accuracy of 0.0001 g.

Single-edge notched bending specimens (SENBs) with dimensions of $2.5 \times 5 \times 30$ mm^3 were used for room-temperature fracture toughness measurements. The notch in the SENBs was prepared by EDM using a Mo wire of 0.18 mm in diameter and without any fatigue precracking. The depth of the notch was 2.4–2.5 mm. The crosshead speed during the bending tests was 0.2 mm/min. Three specimens were tested and the average value was employed for the room-temperature fracture toughness of each specimen condition. The Vickers microhardness of the specimens was measured using an HXP-1000TM hardness machine with a load of 0.98 N. The microhardness values were the average of at least 10 indentations.

X-ray diffraction analysis (XRD, Panalytical X'Pert PRO) was used to identify the constituent phases of both the specimens under as-cast condition and their scales formed upon oxidation at 1250 °C. The microstructure of all the specimens was observed by scanning electron microscopy (SEM, Zeiss Supra-55), and the chemical compositions of their constituent phases were analyzed by electron probe microanalysis (EPMA, JXA8100) or energy dispersive X-ray spectroscopy (EDS, Inca X-sight).

The compound BN and the pure element ingots were used as standards for analyzing the concentrations of B and other elements in the specimens by EPMA analysis. The analysis of B in phases in the microstructure was done using voltage and beam current of 9 kV and 30 nA, respectively. In order to reduce the influence of neighboring phases on the analyzing composition, the testing points were chosen within phase areas of larger size (both the width and length of the analyzed phase were larger than 5 μm). At least five analyses were performed for each phase present in the specimens. Measurements of the area fractions of constituent phases were performed using Image-Pro Plus version 6.0 high resolution imaging analysis software. At least 3 BSE images at the same magnification (×200) were used for each condition and the average value was calculated.

3. Results and discussion

3.1. Microstructure of the alloys

Fig. 1 shows the XRD patterns of Nb silicide based ultrahigh temperature alloys with different B contents. It can be seen that the constituent phases of 0B or 2B alloy were mainly Nbss and $(Nb,X)_5Si_3$. The $(Nb,X)_5Si_3$ phase was found to be either $\alpha(Nb,X)_5Si_3$ in 0B alloy or $\gamma(Nb,X)_5Si_3$ in 2B alloy. The constituent phases of 5B and 10B alloys were mainly Nbss, $\gamma(Nb,X)_5Si_3$ and $(Nb,X)_3Si$.

Fig. 2 shows the backscattered electron (BSE) images of the alloys with different B contents. Four Nb silicide based ultrahigh temperature alloys can all be classified as hypereutectic ones as the primary silicides were present in their microstructure. However, the microstructure of the alloys was obviously changed with increase in B content (Fig. 2). Table 1 gives the chemical compositions of the constituent phases present in these four alloys. According to the SEM, EPMA and XRD results, the microstructure of 0B alloy was mainly composed of primary $\alpha(Nb,X)_5Si_3$ blocks (dark phase, exhibiting faceted morphology), Nbss dendrites (white phase) and Nbss/$\alpha(Nb,X)_5Si_3$ eutectic (Fig. 2a and b). After adding 2 at% B, the formation of $\alpha(Nb,X)_5Si_3$ was completely suppressed, and the microstructure of 2B alloy mainly consisted of primary $\gamma(Nb,X)_5Si_3$ blocks (showing hexagonal morphology), Nbss dendrites and Nbss/$\gamma(Nb,X)_5Si_3$ eutectic (Fig. 2c and d).

The microstructure of 5B or 10B alloy was mainly comprised of primary $\gamma(Nb,X)_5Si_3$ and $(Nb,X)_3Si$ blocks, Nbss dendrites and Nbss/$\gamma(Nb,X)_5Si_3$ eutectic, as shown in Fig. 2e–h. The primary $\gamma(Nb,X)_5Si_3$ (dark phase, exhibiting hexagonal morphology) possessed higher Ti, Hf and Al concentrations than those of primary $(Nb,X)_3Si$ (gray phase, showing irregular morphology) (Table 1). However, the element B was found to be mainly dissolved in $(Nb,X)_3Si$ (~9.4 and ~12.0 at% in 5B and 10B alloys, respectively) and only ~1.3 and ~2.1 at% in $\gamma(Nb,X)_5Si_3$ in these two alloys, respectively. In addition, a certain amount of black regions were observed to exist in the connecting areas between Nbss/$\gamma(Nb,X)_5Si_3$ eutectic

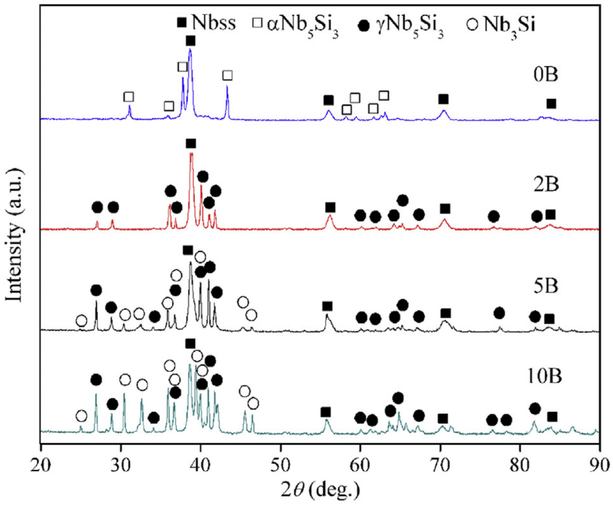

Fig. 1. XRD patterns of the alloys.